

# Experimental validation and docking studies of flavone derivatives on aldose reductase involved in diabetic retinopathy, neuropathy, and nephropathy

Pagadala Nataraj Sekhar · P. B. Kavi Kishor · P. K. Zubaidha ·  
A. M. Hashmi · T. A. Kadam · Lakkireddy Anandareddy · Marc De Maeyer ·  
K. Praveen Kumar · B. Vijaya Bhaskar · T. Munichandrababu ·  
G. Jayasree · P. V. B. S. Narayana · G. Gyananath

Received: 24 December 2009 / Accepted: 16 August 2010 / Published online: 16 September 2010  
© Springer Science+Business Media, LLC 2010

**Abstract** The enzyme aldoreductase which plays an important role in pathogenesis of diabetic retinopathy, neuropathy, and nephropathy was purified from bovine lens, and its inhibitory activity was studied with the synthesized flavone derivatives 1-(2-hydroxyphenyl)ethanone as the starting material. Experimental study revealed that 2-chloroflavone shows less inhibitory activity of 60–70% than other flavones used in the study. To validate experimental results computationally, docking studies of new flavone derivatives synthesized were performed with the enzyme aldose reductase, and the results indicate that 3-iodo, 4-methyl, 5-chloroflavone and 2-chloroflavone bind with higher and lesser affinities.

Docking studies with site directed mutagenesis of Val47Ile, Tyr48His, Pro121Phe, Trp219Tyr, Cys298Ala, Leu300Pro, Ser302Arg, and Cys303Asp of the enzyme altered the inhibition activity of aldose reductase. The regression value ( $R^2$ ) of 0.81 between the docking scores of the known inhibitors and the experimental  $\log IC_{50}$  indicates the reliability of the docking studies. Biological activity and carcinogenic properties predict that 3-iodo, 4-methyl, 5-chloroflavone is the best flavone inhibitor against aldose reductase.

**Keywords** Aldose reductase · Flavones · Docking

P. Nataraj Sekhar (✉) · P. B. Kavi Kishor · L. Anandareddy  
Department of Genetics, Osmania University,  
Hyderabad 500 007, India  
e-mail: nattu251@rediffmail.com

P. K. Zubaidha · A. M. Hashmi  
School of Chemical Sciences, S. R. T. M. University,  
Nanded 431 606, India

T. A. Kadam · G. Gyananath  
School of Life Sciences, S. R. T. M. University,  
Nanded 431 606, India

M. De Maeyer  
Laboratory of Biomolecular Modelling, Division Biochemistry,  
Molecular and Structural Biology, Department of Chemistry,  
Katholieke University, Leuven, Belgium

K. Praveen Kumar · B. Vijaya Bhaskar · T. Munichandrababu  
Sri Venkateswara University, Tirupathi 517 501, India

G. Jayasree  
Srinidhi Institute of Science and Technology,  
Hyderabad 500 007, India

P. V. B. S. Narayana  
CARISM, SASTRA University, Thanjavur, India

## Introduction

Aldose reductase is believed to be of primary importance in the development of severe degenerative complications of diabetes mellitus, through its ability to reduce excess D-glucose into D-sorbitol in non-insulin dependent tissues (Larson *et al.*, 1988). Aldose reductase has been shown to act on a wide range of substrates in vitro, such as aldehydes, aldoses, and corticosteroids, but it is most effective on steroid hormones (Wermuth and Monder, 1983), as confirmed by several reports (Warren *et al.*, 1993). This NADPH-dependent enzyme reduces carbonyl oxygen to a hydroxyl in an ordered 'bi-bi' mechanism, in which NADPH is bound first and NADP<sup>+</sup> is released last. Like all other NAD(P)<sup>+</sup>-dependent enzymatic reactions described to date, this reduction is stereospecific with respect to the coenzyme. Upon formation of the enzyme-coenzyme-substrate tertiary complex, a hydride is transferred from C4 carbon atom of the nicotinamide ring (hydrogen 4-pro-R of the A-face of the ring) of NADPH to the carbonyl carbon of the substrate while a proton is provided by the enzyme to the carbonyl oxygen (Hoffman *et al.*, 1980). In the presence of NADPH, the enzyme converts glucose to

sorbitol, which is only slowly metabolized to fructose by sorbitol dehydrogenase, the other enzyme in the pathway, with concurrent reduction of  $\text{NAD}^+$ . It has been shown that the oxidation of sorbitol catalyzed by sorbitol dehydrogenase increases the ratio of  $\text{NADH}:\text{NAD}^+$ , resulting in an increased lactate: pyruvate ratio and pseudohypoxia (Williamson *et al.*, 1993). Enhanced flux of glucose via polyol pathway under hyperglycemic conditions may play an important role in the pathogenesis of diabetic retinopathy, neuropathy, and nephropathy (Bhatnagar and Srivastava, 1992). Thus, AR represents an attractive pharmacological target to interrupt the polyol pathway and hence delay in the onset/severity of these late diabetic complications (Yabe-Nishimura, 1998). A number of aldose reductase inhibitors (ARIs) were developed and tested in patients for the treatment of such complications (Gabbay *et al.*, 1979; Judzewitsch *et al.*, 1983; Dvornik, 1987; Masson and Boulton, 1990). Presently, none of these drugs are therapeutically effective due to their side effects, non-specificity, and inhibition of other members of the aldo-keto reductase family (Martyn *et al.*, 1987; O'Brien *et al.*, 1982; Poulosom, 1986). Though a broad variety of aldose reductase inhibitors (ARIs) were synthetically developed from lead compounds obtained from in vitro screening studies, very few compounds have qualified for clinical trials (Narayanan, 1993; Nakai *et al.*, 1985). Crystallographic, modeling, and structure–function studies of AR have yielded various classes of ARIs with potent inhibitory activity. The drug tolrestat which was launched in 1989 was withdrawn in 1996, principally due to its low efficacy. Of the newer compounds, zopolrestat and zenarestat were also withdrawn from clinical trials (Mylari *et al.*, 1991). At present, only epalrestat which was developed by Ono and launched into the Japanese market in 1992 is still available (Kawamura *et al.*, 1997). As a group, flavonoids are among the most potent naturally occurring ARIs (Varma *et al.*, 1975). As part of the ongoing project some of the new flavones were screened for their AR inhibitory activity. Considering that pig AR shares 90% sequence identity with bovine AR, this study was carried out in search for the new potential aldose reductase inhibitors that are useful for the treatment of diabetic complications. Hence, docking studies were carried out with the newly derived and known inhibitors on the crystal structure of aldoreductase and their binding affinities calculated.

## Materials and methods

### Synthesis of flavone

#### *Preparation of O-benzoyloxyacetophenone*

The 0.25 mol of *O*-hydroxy acetophenone was placed in a flask and 0.35 mol of benzoyl chloride and 50 ml of dry,

redistilled pyridine were added. The contents in the mixture were shaken until the contents become warm. After 20 min, pour the reaction mixture with stirring into 1 M HCl containing crushed ice. Filter off the product with suction and wash it with 50 ml of ice-cold methanol and then with 50 ml of water. Recrystallise from methanol, cooling in ice before collecting the purified product by filtration. Report the yield and melting point.

#### *Preparation of O-hydroxydibenzoylmethane*

Dissolve (0.2 mol) benzoyloxyacetophenone in dry pyridine in a 1-liter bolt-necked flask and heat the solution to  $50^\circ\text{C}$ . Add with mechanical stirring (0.3 mol) of potassium hydroxide which has been powdered rapidly in a mortar preheated in oven at  $100^\circ\text{C}$ . Continue to stir by hand for 15 min, until the separation of the yellow potassium salt of the product makes mechanical stirring impossible. Cool the reaction mixture to room temperature and acidify it by 10% aqueous acetic acid. Collect the pale yellow solid by suction filtration and dry it in oven at  $50^\circ\text{C}$ . Record the yield of *O*-hydroxydibenzoylmethane and melting point.

#### *Preparation of flavones*

Dissolve 0.15 mol of *O*-hydroxydibenzoylmethane in a flask containing glacial acetic acid and concentrated sulfuric acid. Attach a reflux condenser and heat the mixture on a boiling water bath shaking for 1 h. Pour the reaction mixture with stirring in a crushed ice, and allow the ice to melt. Filter off the flavone which has been separated and wash it with water until the washings are no longer acidic and dry in a oven at  $50^\circ\text{C}$ . Report the yield and melting point at  $50^\circ\text{C}$ . Pathway for the synthesis of the flavone is shown in Fig. 1.

#### *Isolation and purification of aldose reductase from bovine lens*

Bovine lenses were obtained from a local abattoir soon after slaughtering and were frozen until further use. Lenses (30–60 g) were homogenized in a volume of cold buffer in a homogenizer and centrifuged at  $10,000 \times g$  for 20 min to remove insoluble material. Ammonium sulfate was added to the supernatant fluid to 40% saturation. The thick suspension was allowed to stand with occasional stirring for 15 min to ensure complete precipitation. Further, this was centrifuged and the precipitate was discarded. Additional inert protein was removed by increasing the ammonium sulfate concentration from 50 to 75% saturation and the mixture was then centrifuged. The precipitated enzyme was redissolved in 0.05 M sodium chloride and dialyzed overnight against 0.05 M sodium chloride to increase the

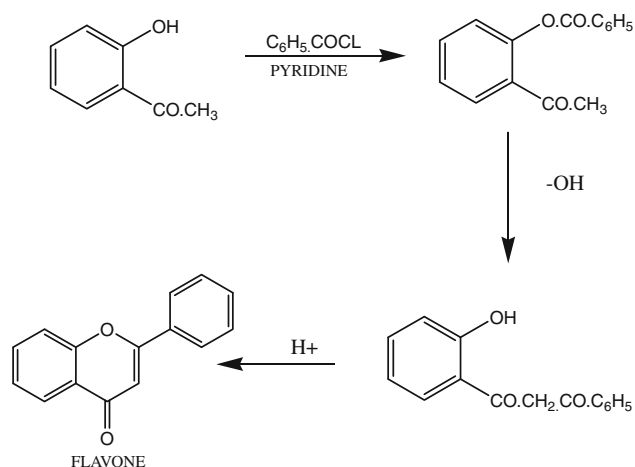


**Fig. 1** Pathway for the synthesis of flavone using 1-(2-hydroxyphenyl)ethanone as the starting material in the presence of pyridine and benzoyl chloride

specific activity of the purified enzyme. Purification of aldose reductase was carried by column chromatography on DEAE-cellulose column (2 × 25 cm) by equilibration with 0.01 M phosphate buffer and then the dialyzed enzyme preparation was adsorbed on the column. Further, it was washed with 0.01 M phosphate buffer until the absorbance at 280 nm of the elute was <0.1. The elution of the enzyme was accomplished with a linear gradient. The inhibition was studied by addition of coenzyme and was monitored on a UV–visible double-beam spectrophotometer (Schimazdu make) at 340 nm.

#### Measurement of aldose reductase activity

DL-glyceraldehydes, NADPH, and quercetin were purchased from Sigma-Aldrich Chemicals (Germany), whereas DEAE-cellulose from Bangalore Genie Pvt. Ltd. (India). Protein concentration was determined using standard calibration curve of bovine serum albumin. Bovine lens for the isolation and purification of aldose reductase were obtained from freshly slaughtered animals. Melting points were determined in open capillaries on a Mettler FP 51 apparatus and are uncorrected. IR spectra were taken on FT-IR Shimadzu Perkin Elmer 1310 Infrared spectrophotometer. HNMR spectra were recorded on Varian Gemini (200 MHz) spectrophotometer, and TMS was used as internal standard. All flavones were prepared by reported procedure. AR activity was assayed according to the method described by Hayman and Kinoshita (1965). The incubation mixture contained phosphate buffer of 0.067 M (final pH of the reaction mixture was 6.2), lithium sulfate of 0.2 M, NADPH of  $5 \times 10^{-5}$  M, enzyme solution of 100  $\mu$ l, DL-glyceraldehydes of  $5 \times 10^{-4}$  M, and distilled water to a final volume of 3 ml with (24  $\mu$ M) or without flavone. Each flavonoid compound was dissolved in

dimethyl sulfoxide to get 1.8 mM concentration. The blank contained all the reagents except DL-glyceraldehydes. The reaction was initiated by adding NADPH and was followed by UV–visible double-beam spectrophotometer at 340 nm. A unit of activity was defined as change in absorbance of 0.001 per minute.

#### Protein–ligand docking

The substrate, product, and inhibitors including all hydrogen atoms were built and optimized with chemsketch software suite. Crystal structure of aldoreductase (PDB: 1AH0) from pig having 90% similarity with aldoreductase from bovine lens was used for docking study. Extremely Fast Rigid Exhaustive Docking (FRED) version 2.1 was used for docking (Open Eye Scientific Software, Santa Fe, NM). FRED docking roughly consists of two steps: shape fitting and optimization. During shape fitting, the ligand was placed into a 0.5 Å-resolution grid box encompassing all active site atoms (including hydrogen's) using a smooth Gaussian potential (McGann *et al.*, 2003). A series of three optimization filters were then processed, which consists of (1) refining the position of hydroxyl hydrogen atoms of the ligand, (2) rigid body optimization, and (3) optimization of the ligand pose in the dihedral angle space. In the optimization step, four scoring functions were available: Gaussian shape scoring (McGann *et al.*, 2003), Chemscore (Eldridge *et al.*, 1997), PLP (Gehlhaar *et al.*, 1995), and Screenscore (Stahl and Rarey, 2001). Preliminary docking trials indicated us to select Chemscore for the 3-optimization filters. This program generates an ensemble of different rigid body orientations (poses) for each compound conformer within the binding pocket and then passes each molecule against a negative image of the binding site. Poses clashing with this 'bump map' are eliminated. Poses surviving the bump test are then scored and ranked with a Gaussian shape function. We defined the binding pocket using the ligand-free protein structure and a box enclosing the binding site. This box was defined by extending the size of a ligand by 4 Å (add box parameter of FRED). One unique pose for each of the best-scored compounds was saved for the subsequent steps. The compounds used for docking were converted in 3D with OMEGA which has previously been shown to select a conformation similar to that of the X-ray input when using appropriate parameters (Bostrom *et al.*, 2003) (same protocol as above; Open Eye Scientific Software, Santa Fe, NM). To this set, the coenzyme (generation of multiconformer with Omega) corresponding to the modeled protein was added. It is an implementation of multiconformer docking, meaning that a conformational search of the ligand was first carried out, and all relevant low-energy conformations were then rigidly placed in the binding site. This two-step process allows

only the remaining six rotational and translational degrees of freedom for the rigid conformer to be considered. The FRED process uses a series of shape-based filters, and the default scoring function is based on Gaussian shape fitting (Schulz-Gasch and Stahl, 2003).

### Bioactivity

The bioavailability of compounds was assessed using adsorption, distribution, metabolism, elimination (ADME) prediction methods. Compounds were also tested to the Lipinski's Rule of Five using MOLINSPIRATION. The polar surface areas (PSA) were calculated since it is another key property linked to drug absorption, including intestinal absorption, bioavailability, Caco-2 permeability, and blood-brain barrier penetration. Thus, passively absorbed molecules with a PSA > 140 Å<sup>2</sup> are thought to have low oral bioavailability. Drug likeliness was also calculated using OSIRIS server, which is based on a list of about 5,300 distinct substructure fragments created by 3,300 traded drugs as well as 15,000 commercially available chemicals yielding a complete list of all available fragments with associated drug-likeliness. The drug score combines drug-likeliness, cLogP, logS, molecular weight, and toxicity risks as a total value which may be used to judge the compound's overall potential to qualify for a drug.

## Results

### Activity of the enzyme

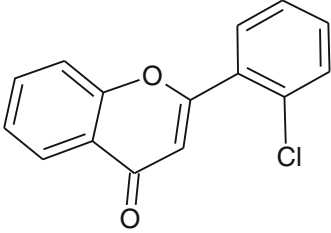
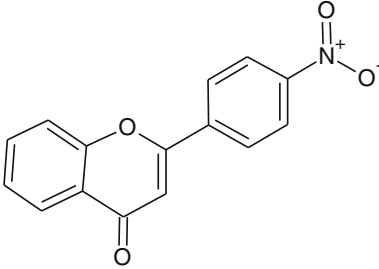
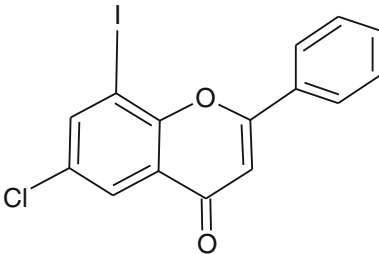
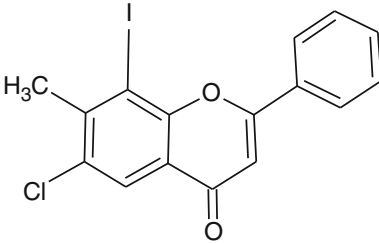
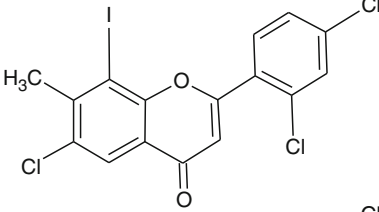
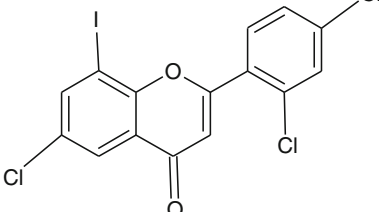
The flavones 3-iodo, 4-chloro, 5-chloroflavone, 2,4-dichloroflavone, 3-iodo, 4-methyl, 5-chloro, 2,4-dichloroflavone, 3-iodo, 5-chloro, 2,4-dichloroflavone inhibited 80–90%, 3-iodo, 5-chloroflavone 70–80%; 4-nitroflavone and 2-chloroflavone 60–70% of the activity (Table 1).

### Docking studies of the substrate, product, and flavone derivatives

Docking of the substrate, product, and flavone derivatives with the active site of the enzyme aldoreductase (PDB: 1AH0) was performed using FRED v 2.0, which is based on rigid body shape-fitting. To understand interactions between the enzyme–substrate, product, and inhibitors, enzyme–product, and enzyme–inhibitor complexes were generated using the OPENEYE software suite (Figs. 2, 3, 4). Table 2 shows the docking scores of substrate and product including the Chemgauss score, Chemscore, PLP score, Screenscore, and Shapeguass score for all the residues in the active sites of enzyme. From Table 2 it was found that the glucose is binding with higher affinity

(−376.62) (Fig. 2a) compared to sorbitol (−293.37) (Fig. 2b). From Table 2 it is evident that enzyme–substrate complex has large favorable total docking scores of −33.92 using Chemgauss, −10.77 of Chemscore, −30.88 of PLP score, −70.33 of Screenscore, and −230.74 of Shapeguass score. Docking studies of the inhibitors with the active site of aldose reductase showed that 3-iodo, 4-methyl, 5-chloroflavone binds with higher affinity (−688.46) (Fig. 3a) compared to 3-iodo, 5-chloro, 2,4-dichloroflavone (−612.33) (Fig. 3b), 3-iodo, 4-methyl, 5 chloro, 2,4, dichloroflavone (−520.3) (Fig. 3c), 4-nitroflavone (−634.74) (Fig. 3d), 3-iodo, 5-chloroflavone (−670.58) (Fig. 3e), and 2-chloroflavone (−575.68) (Fig. 3f). The experimental results also show that 3-iodo, 4-chloro, 5-chloroflavone, 3-iodo, 5-chloro, 2,4-dichloroflavone, 3-iodo, 4-methyl, 5 chloro, 2,4, dichloroflavone inhibit 80–90% of the enzyme activity (Table 1), thus correlating exactly with our docking studies (Table 3). The only inhibitor, which is deviating with experimental results, is 4-nitroflavone, which exhibited 60–70% of enzyme inhibition. This flavone shows higher affinity compared to 3-iodo, 4-methyl, 5-chloro, 2,4-dichloroflavone and 3-iodo, 5-chloro, 2,4-dichloroflavone with the crystal structure of pig aldose reductase. Hydrogen bonding and hydrophobic interactions were clearly seen between O17 atom of 3-iodo, 4-methyl, 5-chloro, 2,4-dichloroflavone with nitrogen atoms of Ala299 and Leu300. Also, interaction of O16 of 3-iodo, 5-chloro, 2,4-dichloroflavone and 2,4-dichloroflavone with nitrogen atoms of Ala299 and Leu300 with two hydrogen bonding in addition to seven hydrophobic interactions with Trp20, Trp79, Trp111, Phe122, Leu124, Trp219, and Leu300. The O17 atom of 3-iodo, 4-chloro, 5-chloroflavone showed hydrogen bonding interactions with nitrogen atoms of Ala299 and Leu300, O16 atoms of 3-iodo, 5-chloroflavone and 2-chloroflavone displayed its interaction with nitrogen atoms of Ala299 and Leu300 and O20 of 4-nitroflavone shows two hydrogen bonding with nitrogen atoms of Leu300 and Met301 residues of the active site predicting that the hydrophobic ring system of these inhibitors gets trapped tightly in a pocket formed by Trp111, Leu300, and Phe122 and are shared by both the active site between Trp20 and Trp111-Phe122 and specificity pocket between Trp111, Leu300, and Phe122. These results indicate that benzene ring of the inhibitors was located within hydrophobic contacts with the side chains of Trp20, Val47, Phe122, Phe121, Trp219, and Leu300. These interactions were suggested to be responsible for the high affinity and selectivity of inhibitors for aldose reductase as shown in Table 3. These studies also revealed that Ala299 and Leu300 are important anchoring residues for the inhibitor binding (Table 3). To evaluate these results, docking studies of the inhibitors with site-directed mutagenesis were carried out with the crystal structure of

**Table 1** Synthesized flavone derivatives used in the study for the inhibition activity of aldose reductase

| S. no. | Compound                                       | Chemical structure   | Enzyme inhibition |
|--------|--|--|-------------------|
| 1      | 2-Chloroflavone                                |    | +                 |
| 2      | 4-Nitroflavone                                 |    | +                 |
| 3      | 3-Iodo-5-chloroflavone                         |   | ++                |
| 4      | 3-Iodo, 4-methyl, 5-chloroflavone              |  | +++               |
| 5      | 3-Iodo, 4-methyl, 5-chloro,2,4-dichloroflavone |  | +++               |
| 6      | 3-Iodo, 5-chloro,2,4-dichloroflavone           |  | +++               |

+: 60–70% inhibition

++: 70–80% Inhibition

+++: 80–90% Inhibition

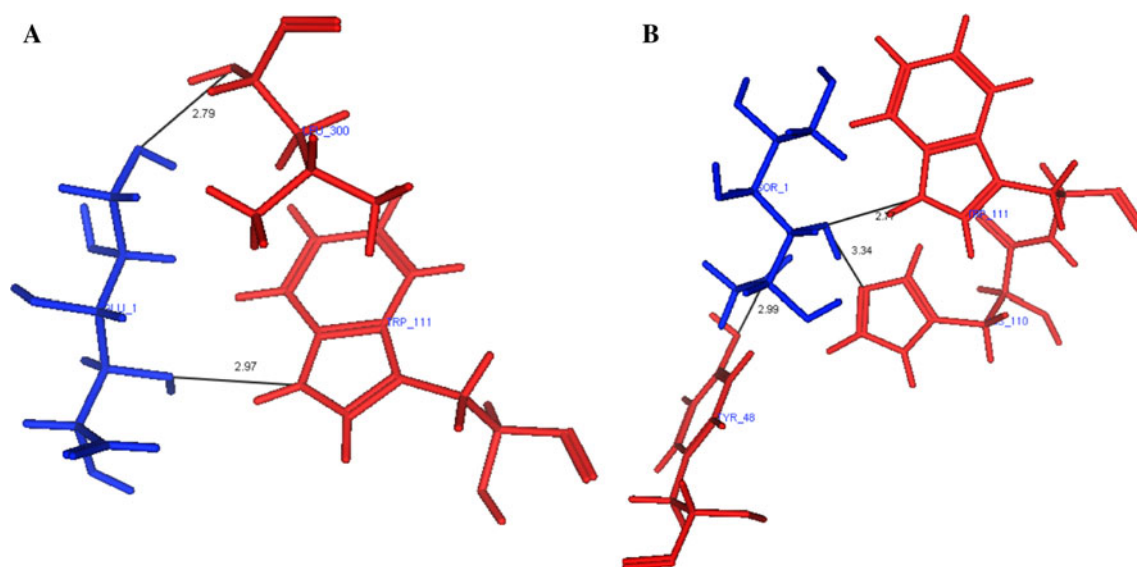
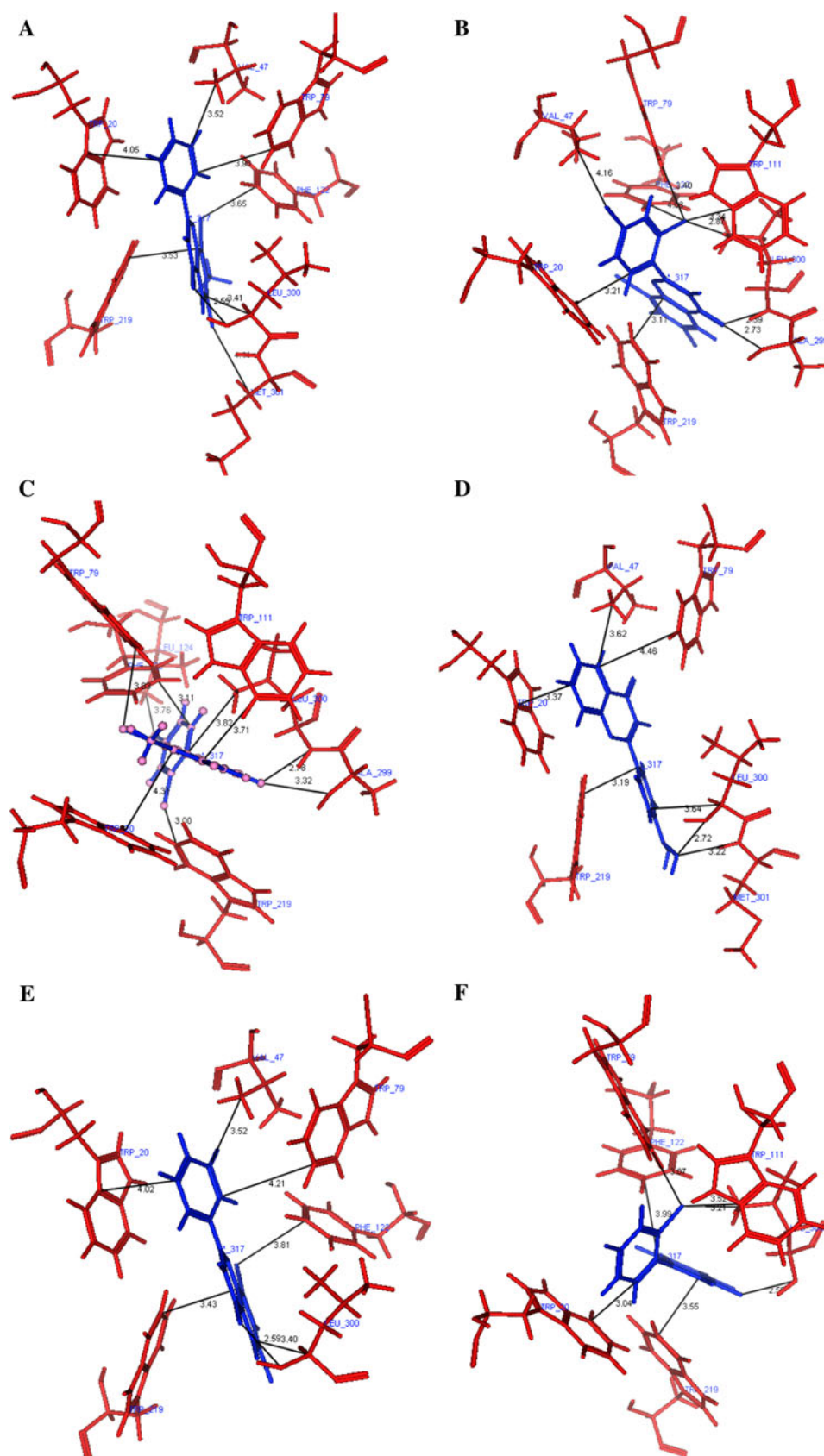


**Fig. 2** Binding of glucose (**a**) and sorbitol (**b**) in the active site of aldoreductase. Substrate, product and residue labels are represented in *blue color* and protein is represented in *red color*. Distances in angstroms are represented in *black lines* (Color figure online)

pig aldoreductase. Based on the molecular structure and reaction mechanisms, active site residues in the hydrophobic pocket were hypothesized to be important for the reaction. Thus, we selected for mutagenesis those amino acids that are thought to be important for the inhibitor binding and hydrophobic pocket formation. Mutation of Val47 to Ile (PDB: 2PD5) which caps the catalytic site and accommodates between the aromatic moieties of Tyr48 and Phe122 to isoleucine pushes the neighboring Phe121 side chain slightly out of place compared to wild type. This resulted in the loss of activity of 2-chloroflavone; 3-iodo, 5-chloro, 2,4-dichloroflavone and 4-nitroflavone with the docking scores of  $-569.91$ ,  $-606.22$ , and  $-630.99$  but exhibited good affinity against 2,4-dichloroflavone, 3-iodo, 4-chloro, 5-chloroflavone, 3-iodo, 4-methyl, 5-chloro, 2,4-dichloroflavone, 3-iodo, 5-chloroflavone compared to wild type (Steuber *et al.*, 2008) (Table 3). Mutation of Tyr48 to His (PDB: 2ACU) involved in proton donor, functioning as a general acid catalyst to facilitate the hydride transfer from NADPH to the carbonyl carbon of the substrate to His altered both the hydrophobic properties and steric bulk of the residue. This resulted in partially retained hydrogen bonding of the hydroxyl moiety in an almost complete loss of activity of 2-chloroflavone and 3-iodo, 4-chloro, 5-chloroflavone compared to wild type protein (Bohren *et al.*, 1994). Phe121, located close to Val47 and involved in integrity, dynamics and water accessibility of the sub-pocket between Phe122 and Tyr48, when mutated to Pro121 (PDB: 2PDB), showed no loss of activity of these inhibitors compared to wild type. This

shows that ligands occupy both the specificity pocket and sub-pocket near Val47-Tyr48 and exhibit no greater decrease in affinity with respect to F121P (Steuber *et al.*, 2008). Consistent with our hypothesis, mutation of Trp219Tyr (PDB: 2IPW) resulted in complete loss of activity of these inhibitors due to loss of hydrophobic contributions (Brownlee *et al.*, 2006). Mutation of Cys298Ala (PDB: 2IPW) also resulted in the loss of activity of the inhibitors which create a new pocket for the chlorine moieties to bind due to lack of cysteine sulfhydryl groups. Replacing Cys298 with a smaller amino acid such as glycine may change the reactivity due to the size of hydrophobic pocket. Leu300 in C-terminal loop responsible for open and closed states of the protein when mutated to proline changed the dynamic properties of the loop region and disqualified the backbone nitrogen for hydrogen bonding, but did not change the activity of flavones expect 3-iodo, 4-chloro, 5-chloroflavone and 3-iodo, 5-chloroflavone compared to wild type (Brownlee *et al.*, 2006). Mutation of Ser302Arg (PDB: 2PDM) resulted in shifting the backbone regions of Leu301 and Arg302 away from Val130. This avoids close contacts with the arginine side chain and reduces the activity of 2-chloroflavone, 3-iodo, 5-chloroflavone and 4-nitroflavone with docking scores of  $-574.06$ ,  $-667.85$ , and  $-632.76$ , respectively (Steuber *et al.*, 2008). Finally, mutation of Cys303Asp (PDB: 2PDQ) resulted in loss of activity of these inhibitors compared to wild type and other mutants (Steuber *et al.*, 2008) (Table 3). Based on the results from the mutagenesis, it appears that these active site residues have different roles (Table 4).

**Fig. 3** Binding of 3-iodo, 4-methyl, 5-chloroflavone (**a**), 3-iodo, 5-chloro, 2,4-dichloroflavone (**b**), 3-iodo, 4-methyl, 5 chloro, 2,4, dichloro flavone (**c**), 4-nitroflavone (**d**), 3-iodo, 5-chloroflavone (**e**), and 2-chloroflavone (**f**) in the active site of aldoreductase enzyme in the presence of NADPH. Inhibitors and labels are represented in *blue color* and residues represented in *red color*. Distances in angstroms are represented in *black lines* (Color figure online)





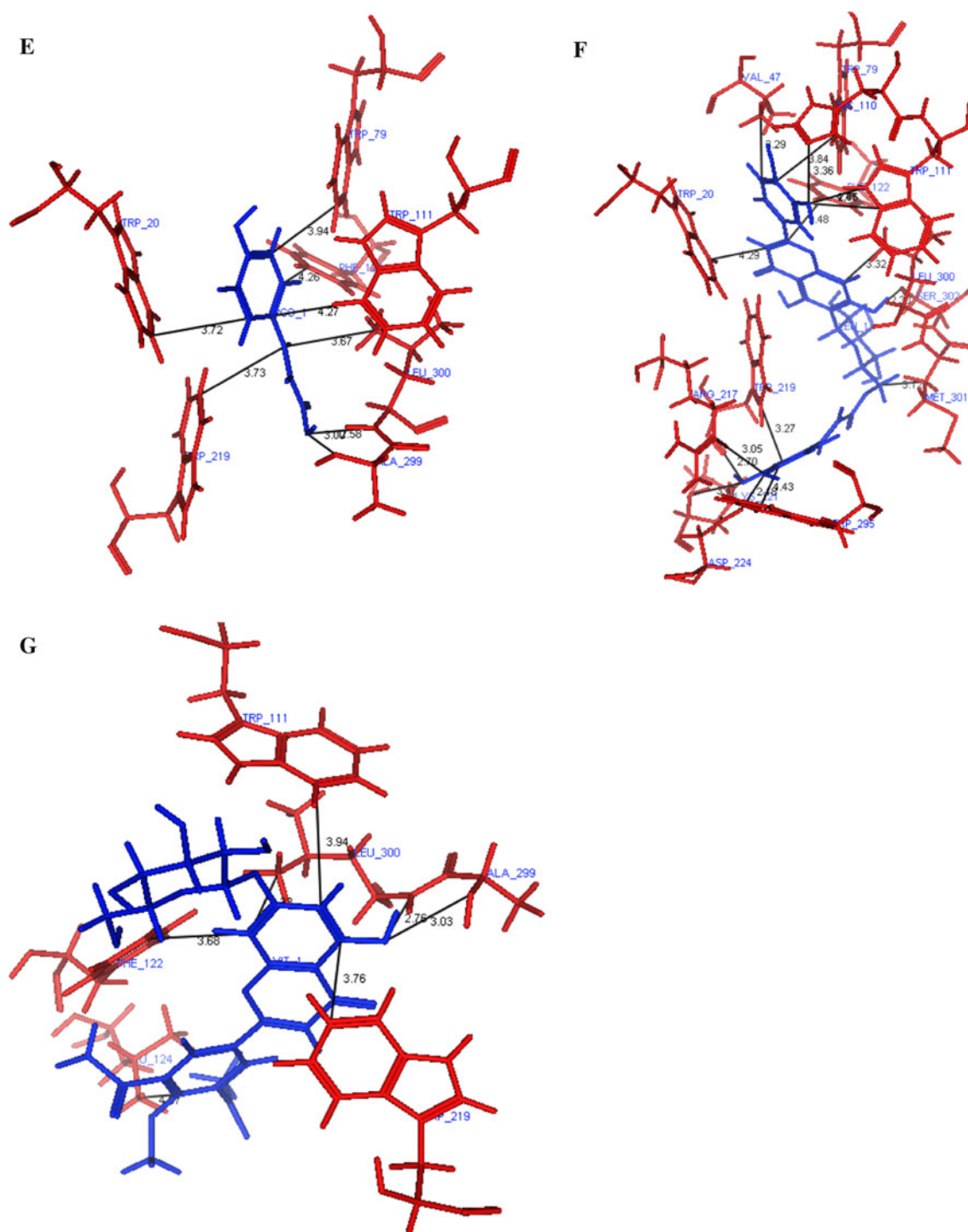


**Fig. 4** continued

nitrogen atoms of His110 (Fig. 4d, e), luteolin 6-*C*-(6'-*O*-*trans*-caffeoylglucoside) displayed eight hydrogen bonding interactions with nitrogen, NH<sub>2</sub>, N $\epsilon$ , and N $\epsilon$ 1 atoms of Ser303, Lys221, Arg217, and Trp297 (Fig. 4f). Vittarilavone showed four hydrogen bonding interactions with

nitrogen, S $\gamma$  N $\epsilon$ 1 and N $\epsilon$ 2 atoms of Met301, Cys298, Trp20, and His110 (Fig. 4g), but tricrin displayed only two hydrogen bonding interactions with nitrogen atoms of Met301 and Ala299 residues, respectively (Fig. 4h; Table 5). Total docking scores calculated are shown in Table 6, and it is

**Table 2** The total scores of Chemguass score, Chemscore score, PLP score, Screenscore, and Shapeguass scores of the best-docked conformations of substrate and product in the active site of aldose reductase

| Ligand   | Chemguass | Chemscore | PLP score | Screenscore | Shapeguass | Total score |
|----------|-----------|-----------|-----------|-------------|------------|-------------|
| Glucose  | -33.92    | -10.77    | -30.86    | -70.33      | -230.74    | -376.62     |
| Sorbitol | -36.34    | -6.4      | -11.62    | -40.59      | -198.42    | -293.37     |

**Table 3** Hydrogen bonding and hydrophobic interactions of the best-docked conformations of the flavone derivatives in the active site of aldose reductase

| Compound  | Hydrogen bonding |           |        | Hydrophobic |           |     |
|---|------------------|-----------|--------|-------------|-----------|-----|
|   | Protein          | Atom-Atom | Lig    | Protein     | Atom-Atom | Lig |
| 3-Iodo, 4-methyl, 5-chloro, 2,4-dichloroflavone | Ala299           | N399-O1   | Lig    | Trp20       | C98-C7    | Lig |
|   | Leu300           | N400-O1   | Lig    | Trp79       | C399-I1   | Lig |
|   |                  |           |        | Trp111      | C568-C10  | Lig |
|   |                  |           |        | Phe122      | C626-C1   | Lig |
|   |                  |           |        | Leu124      | C637-CL1  | Lig |
|   |                  |           |        | Trp219      | 1117-CL3  | Lig |
|   |                  |           |        | Leu300      | 1539-C6   | Lig |
|   |                  |           |        |             |           |     |
|   |                  |           |        |             |           |     |
|   |                  |           |        |             |           |     |
| 3-Iodo, 4-methyl, 5-chloroflavone               | Leu300           | N400-O1   | Lig    | Trp20       | C98-C2    | Lig |
|   |                  |           |        | Val47       | C228-c3   | Lig |
|   |                  |           |        | Trp79       | C399-C5   | Lig |
|   |                  |           |        | Phe122      | C627-I1   | Lig |
|   |                  |           |        | Trp219      | 1118-C8   | Lig |
|   |                  |           |        | Leu300      | 1535-C6   | Lig |
|   |                  |           |        | Met301      | 1543-CL1  | LIG |
| 3-Iodo, 5-chloro, 2,4-dichloroflavone           | Ala299           | N399-O1   | Lig    | Trp20       | C98-C1    | Lig |
|   | Leu300           | N400-O1   | Lig    | Val47       | C228-CL1  | Lig |
|   |                  |           |        | Trp79       | C399-CL3  | Lig |
|   |                  |           |        | Trp111      | C566-CL3  | Lig |
|   |                  |           |        | Phe122      | C627-CL3  | Lig |
|   |                  |           |        | Trp219      | 1117-CL2  | Lig |
| 4-Nitroflavone                                  | Leu300           | N400-O4   | Lig    | Leu212      | 1091-C7   | Lig |
|   | Met301           | N401-O4   | Lig    | Leu228      | 1170-C8   | Lig |
| 3-Iodo, 5-chloroflavone                         | Leu300           | N400-O1   | Lig    | Trp20       | C95-C2    | Lig |
|   |                  |           |        | Val47       | C228-C3   | Lig |
|   |                  |           |        | Trp79       | C398-C3   | Lig |
|   |                  |           |        | Trp219      | 1118-C9   | Lig |
|   |                  |           |        | Leu300      | 1535-C7   | Lig |
| 2-Chloroflavone                                 |                  |           |        | Trp20       | C95-C6    | Lig |
|   |                  |           |        | Val47       | C227-CL1  | Lig |
|   |                  |           |        | Trp79       | C402-C5   | Lig |
|   |                  |           |        | Phe121      | C626-C9   | Lig |
|   |                  |           |        | Phe122      | C635-C1   | Lig |
|   |                  |           |        | Trp219      | 1127-C3   | Lig |
|   |                  |           | Leu300 | 1552-C1     | Lig       |     |

clear from the table that flavones such as isoorientin, vitexin, luteolin 6-*C*-(6'-*O*-*trans*-caffeoylglucoside) and triclin exhibit much stronger aldose reductase inhibition than other compounds exactly correlating with the experimental data

of 1.91, 2.03, 0.0134 and 2.03  $\mu$ M. Of these compounds, luteolin 6-*C*-(6'-*O*-*trans*-caffeoylglucoside) exhibited stronger affinity against aldose reductase activity with the docking score of -829.58 and the inhibitory potency as

**Table 4** Site-directed mutagenesis of the best-docked conformations of flavone derivatives in the active site of aldose reductase

| Compound  | Wild type | Val47Ile | Tyr48His | Pro121Phe | Trp219tyr | Cys298Ala | Leu300Pro | Ser303Arg | Cys303Asp |
|---|-----------|----------|----------|-----------|-----------|-----------|-----------|-----------|-----------|
| 3-Iodo, 4-methyl, 5-chloroflavone               | -688.46   | -687.42  | -685.46  | -688.48   | -360.31   | -679.43   | -651.75   | -688.1    | -688.16   |
| 3-Iodo, 5-chloro,2,4-dichloroflavone            | -612.33   | -606.22  | -638.14  | -612.3    | -373.13   | -601.72   | -644.98   | -612.38   | -612.11   |
| 3-Iodo, 4-methyl, 5-chloro, 2,4-dichloroflavone | -620.3    | -629.97  | -637.89  | -620.4    | -385.66   | -615.01   | -644.04   | -641.56   | -619.53   |
| 3-Iodo, 5-chloroflavone                         | -670.58   | -669     | -678.35  | -670.59   | -331.71   | -660.92   | -622.89   | -667.85   | -670.33   |
| 4-Nitroflavone                                  | -634.74   | -630.99  | -665.6   | -634.88   | -567.34   | -624.91   | -700.31   | -632.76   | -634.59   |
| 2-Chloroflavone                                 | -575.68   | -569.91  | -568.81  | -575.69   | -342.73   | -565.1    | -657.23   | -574.06   | -575.46   |

Total scores are predicted based on Chemguass score, Chemscore score, PLP score, Screenscore, and Shapeguass scores using OPENEYE software

**Table 5** Hydrogen bonding interactions of the known flavonoids predicted using SPDBV software along with their distances in Angstroms

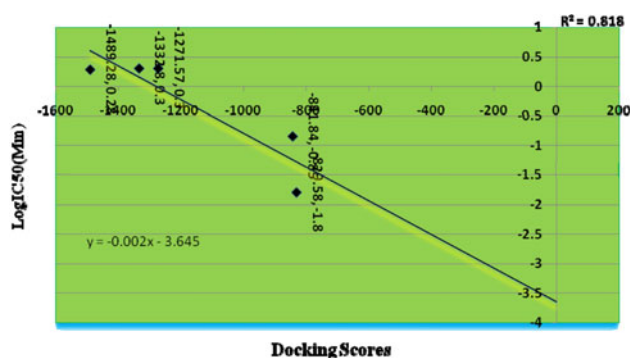
| Compound   | Lig | Atom–Atom          | Protein | Distance (Å) |
|--|-----|--------------------|---------|--------------|
| Isoorientin  | Lig | O28–N              | Ala299  | 2.17         |
|  | Lig | O28–N              | Met301  | 2.94         |
|  | Lig | H32–O $\gamma$     | Ser302  | 3.29         |
| Orientin   | Lig | O22–N              | Leu300  | 2.91         |
|  | Lig | H31–O              | Val47   | 3.10         |
|  | Lig | H27–O7             | NADPH   | 3.35         |
| Vitexin  | Lig | O22–N              | Leu300  | 2.23         |
|  | Lig | O22–N              | Met301  | 3.28         |
| <i>Cis</i> -Coumaric acid  | Lig | O11–N $\epsilon$ 2 | His110  | 2.40         |
|  | Lig | O12–N              | Met301  | 3.35         |
| <i>p</i> -Coumaric acid  | Lig | O11–N $\epsilon$ 2 | His110  | 2.40         |
|  | Lig | O12–N              | Met301  | 3.35         |
| luteolin 6- <i>C</i> -(6'- <i>O</i> - <i>trans</i> -caffeoyl)glucoside | Lig | O39–N              | Ser302  | 2.20         |
|  | Lig | O34–N              | Ser302  | 3.34         |
|  | Lig | O38–N              | Lys221  | 2.58         |
|  | Lig | O38–NH2            | Arg217  | 3.03         |
|  | Lig | O38–N $\epsilon$   | Arg217  | 2.85         |
|  | Lig | O36–NH2            | Arg217  | 3.03         |
|  | Lig | O36–N $\epsilon$   | Arg217  | 2.32         |
| Vittariflavone   | Lig | H36–N $\epsilon$ 1 | Trp297  | 3.23         |
|  | Lig | O27–N              | Met301  | 3.25         |
|  | Lig | O35–SG             | Cys298  | 2.97         |
|  | Lig | H34–N $\epsilon$ 1 | Trp20   | 2.91         |
|  | Lig | H33–N $\epsilon$ 2 | His110  | 2.83         |

expressed by IC<sub>50</sub> value was 0.0134  $\mu$ M. A regression analysis of docking scores and logIC<sub>50</sub> for known flavonoids was carried out and the scatter plot was drawn for wild type (Fig. 5). It was found that the R<sup>2</sup> value for wild type was 0.81 exactly correlate well with the results obtained from experimental data (Jung *et al.*, 2007). Hence, docking results of these inhibitors perhaps can be used as a new pharmacophore for lead generation and optimization of novel aldose reductase inhibitors. The bioactivity of the

molecules predicted using Molsoft server shows (Table 7) 1–2 rotatable bonds, molecular weight in between 200 and 500 with a logP value between -0.2 and 3.2. The drug likeliness of the molecules generated was calculated based on the comparison of the 5,000 marketed drugs (positives) and 10,000 carefully selected non-drug compounds (negatives). It appears from the results that all of the molecules contain positive scores within the range from 0 to 4 (Table 8).

**Table 6** The total scores of Chemguass, Chemscore, PLP, Screenscore, and Shapeguass score of the best-docked conformations of known inhibitors in the active site of aldose reductase

| Compound                                    | Chemguass | Chemscore | PLP score | Screenscore | Shapeguass | Total score | IC <sub>50</sub> (μM) |
|---|-----------|-----------|-----------|-------------|------------|-------------|-----------------------|
| Isoorietin                                  | -75.99    | -22.52    | -67.2     | -151.95     | -477.19    | -794.85     | 1.91                  |
| Orientin                                    | -69.89    | -15       | -49.33    | -130.86     | -447.64    | -712.72     | -                     |
| Vitexin                                     | -64.76    | -26.71    | -51.41    | -139.8      | -430.47    | -713.15     | 2.03                  |
| Cis-coumaric acid                           | -38.86    | -17.1     | -46.49    | -96.02      | -250.43    | -448.9      | -                     |
| p-Coumaric acid                             | -38.86    | -17.1     | -46.49    | -96.02      | -250.43    | -448.9      | 0.14                  |
| Luteolin 6-C-(6'-O-trans-caffeoyl)glucoside | -83.11    | -28.55    | -32.69    | -128.93     | -556.3     | -829.58     | 0.0134                |
| Vittariflavone                              | -79.5     | -11.53    | -45.95    | -123.2      | -530.07    | -790.25     | -                     |
| Tricin                                      | -71.03    | -20.41    | -58.42    | -120.52     | -412.14    | -682.52     | 2.03                  |

**Fig. 5** Correlation of the docking scores of the known inhibitors with their experimental logIC<sub>50</sub> values

## Discussion

Aldoreductase inhibitors have been shown to prevent or delay significantly diabetic complications. Many synthetic inhibitors of the enzyme were tested for their clinical use, albeit with limited success (Raskin and Rosenstock, 1987). Synthetic compounds with diverse structures such as sorbinil, epalrestat, other hydantoin derivatives, and flavonoids from natural origin have been extensively studied and reported to inhibit ALR2 (Beyer-Mears and Cruz, 1985, Terashima *et al.*, 1984, Inagaki *et al.*, 1982). Docking studies of 2-chloroflavone and 4-nitroflavone revealed that chlorine in the second position has higher affinity compared to fourth due to conformational changes

**Table 7** Biological activity values of flavone analogs calculated using MOLINSPIRATION server

| Name  | miLogP | TPSA   | NATOMS | MW      | NON | Nohnh | N violation | N rotb | Volume  |
|---|--------|--------|--------|---------|-----|-------|-------------|--------|---------|
| 2-Chloroflavone                                 | 0.565  | 28.241 | 18     | 257.696 | 2   | 0     | 0           | 1      | 216.624 |
| 4-Nitroflavone                                  | -0.106 | 74.065 | 20     | 268.248 | 5   | 0     | 0           | 2      | 226.423 |
| 3-Iodo, 5-chloroflavone                         | 1.6    | 28.241 | 19     | 383.592 | 2   | 0     | 0           | 1      | 240.615 |
| 3-Iodo, 4-chloro, 5-chloroflavone               | 1.6    | 28.241 | 19     | 383.592 | 2   | 0     | 0           | 1      | 240.615 |
| 3-Iodo, 4-methyl, 5-chloro, 2,4-dichloroflavone | 3.261  | 28.241 | 22     | 466.509 | 2   | 0     | 0           | 1      | 284.247 |
| 3-Iodo, 5-chloro, 2,4-dichloroflavone           | 2.884  | 28.241 | 21     | 452.482 | 2   | 0     | 0           | 1      | 267.680 |

**Table 8** Carcinogenic property values of flavone analogs calculated using OSIRIS server

| Compounds                                       | Muta genic | Tumaro genic | Irritant | Reproductive effect | cLogP | Solubility | MW    | Drug likeness | Drug score |
|---|------------|--------------|----------|---------------------|-------|------------|-------|---------------|------------|
| 2-Chloroflavone                                 | -          | -            | -        | -                   | 4.21  | -4.48      | 256.0 | 2.12          | 0.63       |
| 4-Nitroflavone                                  | +          | +            | -        | -                   | 3.33  | -4.38      | 269   | 2.03          | 0.25       |
| 3-Iodo, 5-chloroflavone                         | -          | -            | -        | -                   | 5.14  | -5.5       | 382.0 | 1.71          | 0.42       |
| 3-Iodo, 4-chloro, 5-chloroflavone               | -          | -            | -        | -                   | 5.45  | -5.84      | 396.0 | 1.36          | 0.36       |
| 3-Iodo, 4-methyl, 5-chloro, 2,4-dichloroflavone | -          | -            | -        | -                   | 6.68  | -7.31      | 464.0 | 3.22          | 0.25       |
| 3-Iodo, 5-chloro, 2,4-dichloroflavone           | -          | -            | -        | -                   | 6.36  | -6.97      | 450.0 | 3.43          | 0.27       |

of the molecule and its hydrophobic interactions with Trp20, Val47, Trp79, Phe121, Phe122, Trp219, and Leu300. These interactions are not seen in the case of 4-nitroflavone that binds with lower affinity. Docking studies of the substrate and its product showed that H9 and H11 of glucose interact with N $\epsilon$ 2 of His110 and O7 of NADPH with distances of 2.66 and 2.41 Å. This indicates that His110 at the bottom of the cavity is an important anchoring residue for the substrate binding during catalysis. Docking analysis also shows that O8 and H12 of sorbitol interact with O7 of NADPH and N $\epsilon$ 2 of His110. This preliminary data along with the list of hydrogen bond interactions between the substrate, product, and residues in the binding cavity clearly indicate that His110 residue is more preferred in binding of the substrate, product, and hydride transfer mechanism. Molecular modeling study performed by Itzstein *et al.* showed that tyr48, His110, and Trp111 are involved in the hydrogen bonding interactions with three substrates, D-xylose, L-xylose, and D-lyxose when His110 was modeled with its N $\epsilon$ 2 atom in the protonated form and N $\delta$ 1 atom in the unprotonated form (De Winter *et al.*, 1995). It was also inferred that reduction of D-glyceraldehyde to glycerol catalyzed by His110 was favored over the reduction process catalyzed by Tyr48. Docking studies with 3-iodo-5-chloroflavone, 3-iodo, 4-methyl, 5-chloroflavone; 3-iodo, 4-methyl, 5-chloro, 2,4-dichloroflavone and 3-iodo, 5-chloro, 2,4-dichloroflavone indicate that methyl in the fourth and chlorine groups in the second and fourth positions of side chain benzene ring are responsible for conformational changes in the active site interacting with higher affinity compared to 3-iodo, 5-chloroflavone. The polar head groups of the inhibitors interacted with Trp20, Val47, Phe122, Phe121, Trp219, and Leu300 adding evidence for the generalized mode of aldose reductase binding. The similarities in the binding modes for the side chain and main chain chlorine, iodine, and carboxyl group flavone derivatives in the active site of aldose reductase are directed by both the hydrophobic ring system and polar head groups of the inhibitors. The binding of these inhibitors is accompanied by a conformational change to the side chain of Leu300 and Phe122 that opens the specificity pocket lined by residues Trp111, Phe113, Phe122, Ala299, and Leu300. These studies show that Ala299 and Leu300 loop regions exhibit a high level of plasticity throughout the known crystal structures, particularly provoked by the less restrained dynamic properties of Phe122, Ala299, and Leu300. These residues populate different rotameric states and thereby produce differently shaped sub-pockets (Urzhumtsev *et al.*, 1996). The inhibitor-binding site is a positively charged anion well formed by Asp43, Lys77, Tyr48, His110, and the nicotinamide ring at the bottom of the active site pocket (Harrison *et al.*, 1994). Replacement of Val47Ile, Tyr48His, Phe121Pro,

Cys298Ala, Leu300Pro, Ser302Arg, Cys303Asp, and double mutation of Ser302Arg and Cys303Asp alters the activity of these inhibitors compared to wild type due to conformational changes and their binding modes. These studies show that these derivatives preferably docked within the specificity pocket of the active site were heavily depend on the degree of halogenation. However, the calculated docking scores were not very similar in all the cases and, rather strikingly, could not be used to tell apart those molecules that were bound in the active site from those bound elsewhere. The preferred orientation found for 3-iodo, 4-methyl, 5-chloroflavone was chosen as the most plausible one for the remaining inhibitors. The different orientations of these inhibitors were thought to arise due to increasing the number of chlorine atoms in the third, fourth and fifth positions in the naphthalene, and bulky size NO<sub>2</sub> group relative to chlorine in the side chain phenyl group, show variations in the docking scores into the rigidly fixed binding site. The docking study of 3-iodo, 4-methyl, 5-chloro, 2,4-dichloroflavone and 3-iodo, 5-chloro, 2,4-dichloroflavone shows that the more heavily halogenated phenyl ring is sandwiched between the indole ring of Trp111 on one side and the side chains of Leu-300 on the other side. Studies also show that the side chain of Leu300 makes a direct contact with the aromatic ring of Trp111 in the native human holoenzyme (PDB code: 1ADS). These hydrophobic interactions are further stabilized by the phenyl ring of Phe-122 whose edge contacts halogenated phenyl ring which are similar to that described for the larger benzothiazole ring of zopolrestat and zenarestat (Kinoshita *et al.*, 2002). The oxygen atom allows a nearly orthogonal orientation of the side chain phenyl ring such that the electronegative chlorine atom in the second phenyl ring makes contact with both Trp-20 and the pyridinium group of NADP<sup>+</sup>. Incorporation of methyl group in the fourth position of 3-iodo, 4-methyl, 5-chloroflavone will likewise result in increase of potency by orientating the molecule in such a way that both chlorine and iodine are in very close contact with protein atoms and engaged in crucial hydrophobic interactions with Phe122 and Met301. The change of binding mode of these flavones derivatives is probably caused by the substitution of the chlorine atoms with NO<sub>2</sub> substituents in the side chain phenyl group in the second position which bring severe steric hindrance because of its big atomic volume. The structural characteristic correlates well with the experimental inhibition activities of inhibitors, which vary a lot under these two binding modes. This is probably because the inhibitors 3-iodo, 4-methyl, 5-chloroflavone, 3-iodo, 4-methyl, 5-chloro, 2,4-dichloroflavone and 3-iodo, 5-chloro, 2,4-dichloroflavone that bear more negative charges because of chlorine atoms than 4-nitroflavone can form more stable hydrogen bonds with active residues, which make the

chlorine binding mode prevail at the binding strength. Furthermore, compared to the 2-chloroflavone which bears chlorine in the fourth position, 3-iodo, 4-methyl, 5-chloro,2,4-dichloroflavone and 3-iodo, 5-chloro,2,4-dichloroflavone cause less severe steric effect and bind to the aldose reductase active pocket effectively due to free rotation of the branched phenyl group. To further understand the inhibition mechanism of flavone derivatives, the substrate (glucose) was docked primarily in the active site of aldose reductase and forms hydrogen bonds with residues TYR48 and HIS110 with carbonyl O atom which is much similar with the inhibitors' binding mode. But glucose has much lower docking score compared with the flavone derivatives, predicting that there is a competitive inhibition of flavone derivatives with more affinity than its substrate in the active site of aldose reductase forming stable hydrogen bonds with Ala299 or Leu300 or both and effectively hinder the proton transfer process to further stop the reduction reaction. Also based on experimental and theoretical studies, it has been established that the reduction of an aldehyde substrate to an alcohol by aldose reductase follows a stepwise mechanism, which consists of a hydride transfer from the nicotinamide ring of coenzyme NADPH and a proton transfer from one of the amino acid residues in the active site (Varnai *et al.*, 1999; Bohren *et al.*, 1994; Grimshaw *et al.*, 1995a, b; Lee *et al.*, 1998; Varnai and Warshel, 2000). According to the residue mutation experiments, the most possible proton donors are TYR48 and protonated HIS110 (Varnai *et al.*, 1999; Lee *et al.*, 1998; Varnai and Warshel, 2000). To further evaluate these docking studies, known flavones were docked such as luteolin 6-*C*-(6'-*O*-*trans*-caffeoylglucoside) was found to exhibit strong aldose reductase activity with the inhibitory potencies as expressed by IC<sub>50</sub> value was 0.0134 mM (Varma and Kinoshita, 1976). This indicated some possible relationships of the structure to the inhibiting potencies of flavones. The hydroxylation in the 4'-position has beneficial effects, and the abolition of the double bond between C-2 and C-3 leads to a decreased inhibition. In support of these findings, the 4'-hydroxyl group of tested compounds was important for showing the inhibition of enzyme activity. Studies indicate that quercetin-like structure of luteolin 6-*C*-(6'-*O*-*trans*-caffeoylglucoside) has stronger inhibition than other flavones (Robison *et al.*, 1989). Higher inhibition of ALR2 activity was reported by Matsuda *et al.* (2002) with the compounds having a catechol moiety at the B ring compared to those of monohydroxyl and pyrogallol moiety (the 3',4',5'-trihydroxyl moiety), while opposite examples were found in flavone 8-glucoside, vitexin [(3, IC<sub>50</sub> = 2.03 mM) and >orientin (2, >10 mM)]. A model with the correlation coefficient ( $r^2$ ) of 0.81 was obtained for five compounds (isorientin, vitexin, *p*-coumaric acid, luteolin 6-*C*-(6'-*O*-

*trans*-caffeoylglucoside), tricetin) using the equation  $Y = -0.0029 \times -3.6458$ . This good correlation between known inhibitors with the crystal structure of pig aldose reductase demonstrates that the binding conformations are reasonable. These studies show that polar head groups of these inhibitors bind in the active site with three hydrophilic centers near the coenzyme and hydrophobic groups bind with different conformational changes in the active site cleft. Docking studies with known and unknown inhibitors along with site directed mutagenesis show that these residues are highly conserved suggesting that the specificity pocket binds to the substrates that are unique to AR. Therefore, the study of these AR-inhibitor complexes and the conformational changes induced by the inhibitors explain the remarkable adaptability of the active site, as well as its specificity for certain inhibitors. Drug likeliness of these molecules was predicted using the OSIRIS server. The data show that molecules contain positive scores within the range from 0 to 0.5 which indicated that the above-mentioned molecules act as drugs and inhibit the activity of aldose reductase. The results also show that 3-iodo, 4-methyl, 5-chloroflavone binds with aldose reductase with high affinity and good drug scores. This indicates that this molecule may be the best inhibitor for aldose reductase. On the basis of docking results, bioavailability scores and carcinogenic properties, it is predicted that the compound 3-iodo, 4-methyl, 5-chloroflavone is the best antidiabetic. Thus, it is hoped that these newly designed molecules hold promise for anti-diabetic activity if tested in animal models.

## Conclusion

Molecular docking studies of flavone derivatives based on the experimental data with aldose reductase reveal that they can form hydrogen bond networks with active residues by using the iodine and chlorine groups. Chlorine in the second position of side chain phenyl group is replaced with NO<sub>2</sub> substituent or without a substituent; an inhibitor shows less binding affinity otherwise the inhibitor shows higher binding affinity. Inhibitors exhibit their anti-aldose reductase activities mainly by occupying the active site. Under these two binding modes, flavone derivatives have different experimental and theoretical inhibition activities to aldose reductase, and the binding mode alteration can be conveniently controlled by introducing methyl, chlorine, and iodine groups or eliminating NO<sub>2</sub> substituent on certain position of inhibitor molecules. Correlation of the docking studies with inhibitory concentration values of the known inhibitors against aldose reductase shows the regression value of 0.81 predicting that these docking studies are reliable. These results show that the synthesized

flavone derivatives used in this study contains some interesting characteristics which make them new kind of promising aldose reductase inhibitors.

**Acknowledgments** The authors are thankful to the Director, Global institute of Biotechnology, Himayatnagar, Hyderabad for his kind support for providing the software necessary to carry out this study.

## References

- Beyer-Mears A, Cruz E (1985) Reversal of diabetic cataract by sorbinil, an aldose reductase inhibitor. *Diabetes* 34:15–21
- Bhatnagar A, Srivastava SK (1992) Aldose reductase: congenial and injurious profiles of an enigmatic enzyme. *Biochem Med Metab Biol* 48:91–121
- Bohren KM, Grimshaw CE, Lai CJ, Harrison DH, Ringe D, Petsko GA, Gabbay KH (1994) Tyrosine-48 is the proton donor and histidine-110 directs substrate stereochemical selectivity in the reduction reaction of human aldose reductase: enzyme kinetics and crystal structure of the Y48H mutant enzyme. *Biochemistry* 33:2021–2032
- Bostrom J, Greenwood JR, Gottfries J (2003) Assessing the performance of OMEGA with respect to retrieving bioactive conformations. *J Mol Graph Model* 21:449–462
- Brownlee JM, Carlson E, Milne AC, Pape E, Harrison DH (2006) Structural and thermodynamic studies of simple aldose reductase inhibitor complexes. *Bioorg Chem* 34:424–444
- De Winter HL, von Itzstein M (1995) Aldose reductase as a target for drug design: molecular modeling calculations on the binding of acyclic sugar substrates to the enzyme. *Biochemistry* 34:8299–8308
- Dvornik D (1987) Hyperglycaemia in the pathogenesis of diabetic complications. In: Porte D (ed) *Aldose reductase inhibition: an approach to the prevention of diabetic complications*. McGraw Hill, New York
- Eldridge MD, Murray CW, Auton TR, Paolini GV, Mee RP (1997) Empirical scoring functions: I. The development of a fast empirical scoring function to estimate the binding affinity of ligands in receptor complexes. *J Comput Aided Mol Des* 11:425–445
- Gabbay KH, Spack N, Loo S, Hirsch HJ, Ackil A (1979) Aldose reductase inhibition: studies with alrestatin. *Metabolism* 28:471–476
- Gehlhaar DK, Verkhivker GM, Rejto PA, Sherman CJ, Fogel DB, Fogel LJ, Freer ST (1995) Molecular recognition of the inhibitor AG-1343 by HIV-1 protease: conformationally flexible docking by evolutionary programming. *Chem Biol* 2:317–324
- Grimshaw CE, Bohren KM, Lai CJ, Gabbay KH (1995a) Human aldose reductase: subtle effects revealed by rapid kinetic studies of the C298A mutant enzyme. *Biochemistry* 34:14366–14373
- Grimshaw CE, Bohren KM, Lai CJ, Gabbay KH (1995b) Human aldose reductase: pK of tyrosine 48 reveals the preferred ionization state for catalysis and inhibition. *Biochemistry* 34:14374–14384
- Harrison DH, Bohren KM, Ringe D, Petsko GA, Gabbay KH (1994) An anion binding site in human aldose reductase: mechanistic implications for the binding of citrate cacodylate and glucose 6-phosphate. *Biochemistry* 33:2011–2020
- Hayman S, Kinoshita H (1965) Isolation and properties of lens aldose reductase. *J Biol Chem* 240:877–882
- Hoffman PL, Wermuth B, Von Wartburg JP (1980) Human brain aldehyde reductases: relationship to succinil semi aldehyde reductase and aldose reductase. *J Neurochem* 35:354–366
- Inagaki K, Miwa I, Yashiro T, Okuda J (1982) Inhibition of aldose reductases from rat and bovine lenses by hydantoin derivatives. *Chem Pharm Bull* 30:3244–3254
- Judzewitsch RG, Jaspán JB, Polonsky KS, Weinberg CR, Halter JB, Halar E, Pfeifer MA, Vukadinovich C, Bernstein L, Schneider M, Liang KL, Gabbay KH, Rubenstein AH, Porte D Jr (1983) Aldose reductase inhibition improves nerve conduction velocity in diabetic patients. *N Engl J Med* 308:119–125
- Jung SH, Lee JM, Lee HJ, Kim CY, Lee EH, Um BH (2007) Aldose reductase and advanced glycation endproducts inhibitory effect of *Phyllostachys nigra*. *Biol Pharm Bull* 30:1569–1572
- Kinoshita T, Miyake H, Fujii T, Takakura S, Goto T (2002) The structure of human recombinant aldose reductase complexed with the potent inhibitor zenarestat. *Acta Crystallogr D* 58:622–626
- Kawamura M, Hamanaka N (1997) Development of epariastat (Kinedak), aldose reductase inhibitor. *J Synth Org Chem Japan* 37:651–657
- Larson ER, Lipinski CA, Sarges R (1988) Medicinal chemistry of aldose reductase inhibitors. *Med Res Rev* 8:159–186
- Lee YS, Hodoscek M, Brooks BR, Kador PF (1998) Catalytic mechanism of aldose reductase studied by the combined potentials of quantum mechanics and molecular mechanics. *Biophys Chem* 70:203–216
- Martyn CN, Reid W, Young RJ, Ewing DJ, Clark BF (1987) Six-month treatment with sorbinil in asymptomatic diabetic neuropathy. Failure to improve abnormal nerve function. *Diabetes* 36:987–990
- Masson EA, Boulton AJ (1990) Aldose reductase inhibitors in the treatment of diabetic neuropathy: a review of the rationale and clinical evidence. *Drugs* 39:190–202
- Matsuda H, Morikawa T, Toguchida I, Yoshikawa M (2002) Structural requirements of flavonoids and related compounds for aldose reductase inhibitory activity. *Chem Pharm Bull* 50:788–795
- McGann MR, Almond HR, Nicholls A, Grant JA, Brown FK (2003) Gaussian docking functions. *Biopolymers* 68:76–90
- Mylari BL, Larson ER, Beyer TA, Zembrowski WJ, Aldinger CE, Dee MF, Siegel TW, Singleton DH (1991) Novel, potent aldose reductase inhibitors: 3,4-dihydro-4-oxo-3-[[5-(trifluoromethyl)-2-benzothiazolyl] methyl]-1-phthalazineacetic acid (zopolrestat) and congeners. *J Med Chem* 34:108–122
- Nakai N, Fujii Y, Kobashi K, Nomura K (1985) Aldose reductase inhibitors: flavonoids alkaloids acetophenones benzophenones and spirohydantoin of chroman. *Arch Biochem Biophys* 239:491–496
- Narayanan S (1993) Aldose reductase and its inhibition in the control of diabetic complications. *Ann Clin Lab Sci* 23:148–158
- O'Brien MM, Schofield PJ, Edwards MR (1982) Inhibition of human brain aldose reductase and hexonate dehydrogenase by alrestatin and sorbinil. *J Neurochem* 39:810–814
- Poulsom R (1986) Inhibition of hexonate dehydrogenase and aldose reductase from bovine retina by sorbinil statil M79175 and valproate. *Biochem Pharmacol* 35:2955–2959
- Raskin P, Rosenstock J (1987) Aldose reductase inhibitors and diabetic complications: a review. *Am J Med* 83:298–306
- Robison WG Jr, Nagata M, Laver N, Hohman TC, Kinoshita JH (1989) Diabetic-like retinopathy in rats prevented with an aldose reductase inhibitor. *Invest Ophthalmol Vis Sci* 30:2285–2292
- Schulz-Gasch T, Stahl M (2003) Binding site characteristics in structure based virtual screening: evaluation of current docking tools. *J Mol Model* 9:47–57
- Stahl M, Rarey M (2001) Detailed analysis of scoring functions for virtual screening. *J Med Chem* 44:1035–1042
- Steuber H, Heine A, Podjarny A, Klebe G (2008) Merging the binding sites of aldose and aldehyde reductase for detection of inhibitor selectivity-determining features. *J Mol Biol* 379:991–1016

- Terashima H, Hama K, Yamamoto R, Tsuboshima M, Kikkawa R, Hatanaka I, Shigeta YJ (1984) Effects of a new aldose reductase inhibitor on various tissues in vitro. *Pharmacol Exp Ther* 229:226–230
- Urzhumtsev AG, Skovoroda TP, Vyu Lunin (1996) A procedure compatible with X-PLOR for the calculation of electron-density maps weighted using an R-free-likelihood based approach. *J Appl Crystallogr* 29:741–744
- Varma SD, Kinoshita JH (1976) Inhibition of lens aldose reductase by flavonoids—their possible role in the prevention of diabetic cataracts. *Biochem Pharmacol* 25:2505–2513
- Varma SD, Mikuni I, Kinoshita JH (1975) Flavonoids as inhibitors of lens aldose reductase. *Science* 188:1215–1216
- Varnai P, Warshel A (2000) Computer simulation studies of the catalytic mechanism of human aldose reductase. *J Am Chem Soc* 122:3849–3860
- Varnai P, Richards WG, Lyne PD (1999) Modelling the catalytic reaction in human aldose reductase. *Proteins* 37:218–227
- Warren JC, Murdock GM, Ma Y, Goodman SR, Zimmer WE (1993) Molecular cloning of testicular 20-hydroxysteroid dehydrogenase. *Biochemistry* 32:1401–1406
- Wermuth B, Monder C (1983) Aldose and aldehyde reductase exhibit isocorticosteroid reductase activity. *Eur J Biochem* 127:279–284
- Williamson JR, Chang K, Frangos M et al (1993) Hyperglycemic pseudohypoxia and diabetic complications. *Diabetes* 42:801–813
- Yabe-Nishimura C (1998) Aldose reductase in glucose toxicity: a potential target for the prevention of diabetic complications. *Pharmacol Rev* 50:21–33